Microscopic imaging as a tool to target spatial and temporal extraction of bioactive compounds through ultrasound intensification

Boutheina Khadhraoui, Anne-Sylvie Fabiano-Tixier, Emmanuel Petitcolas, P. Robinet, R. Imbert, Mohamed El Maataoui, Farid Chemat

Microscopic imaging as a tool to target spatial and temporal extraction of bioactive compounds through ultrasound intensification.

B. Khadhraoui [1-2], A.S. Fabiano-Tixier [2], E. Petitcolas [2],
P. Robinet [1], R. Imbert [1], M. El Maâtaoui [3], F. Chemat [2] *

(1) Laboratoires Arkopharma, laboratoire d'étude des substances naturelles, 06510 Carros, France
(2) Avignon University, INRA, UMR408, GREEN Extraction Team, 84000 Avignon, France
(3) Avignon University, Qualisud UMR95, F-84000 Avignon, France

ABSTRACT

Unravelling a chain of events in ultrasound-assisted extraction (UAE) of bioactive compounds from plants has to start with a detailed description of destructuration at macroscopic and microscopic scale. The present work aims to study the impacts and interactions of UAE on the extreme complexity and diversity of plants structures. Three plant species were selected for their difference in specialized structures and their spatial distribution of secondary metabolites: bitter orange leaf (*C. aurantium* L.), blackcurrant leaf (*R. nigrum* L.), and artichoke leaf (*C. scolymus* L.). Different microscopic techniques (Cyto-histochemistry, stereomicroscopic analysis, Scanning Electron Microscopy (SEM)) have been used to understand the complexity of plant structures and to highlight ultrasound-induced impacts especially on metabolites storage structures, with a neat comparison with conventional "silent" extraction procedure. The main results indicate that spatial UAE impacts are strongly related to plant structures' properties (morphology, thickness, etc.) and particularly to the nature and the chemical constitution of their storage specialized structures. From a temporal point of view, for all studied leaves, observed mechanisms followed a special order according to structures and their mechanical resistance level to ultrasound (US) treatment. Microscopic mapping of metabolites and structures should be considered as a decision tool during UAE to target intensification process.

Keywords: Ultrasound-Assisted Extraction; microscopic observations; mechanism; specialized structures; bioactive compounds.

Corresponding author: Farid CHEMAT (farid.chemat@univ-avignon.fr)

1. Introduction

Plant cells can be considered as highly performant ‘biofactories’ which produce a myriad variety of high-value products including essentially primary metabolites (lipids, proteins, carbohydrates) and secondary metabolites (terpenes, anthocyanins, polyphenols, etc.) [1,2]. Contrarily to primary metabolites, secondary metabolites do not have a vital role for plants; whereas they have a key role in ensuring chemical communication with their environment [1,2]. They also represent a valuable protection against abiotic and biotic conditions [3,4]. The biosynthesis of those compounds is a highly complex process. Primary metabolites are the precursors of secondary metabolites via three principal photosynthetic metabolic processes namely nitrogen metabolism, fatty acid metabolism, and carbohydrate metabolism. Those three basic pathways generate a large variety of secondary metabolites such as flavonoids, tannins, terpenes, anthocyanins, alkaloids, etc.

Secondary metabolites can be stored at all aerial and underground plant parts (leaves, stems, roots, etc.). Moreover, plants possess several specialized storage structures which can be found in all plant parts [5]. Two major classes of these specialized structures can be distinguished according to their localization [6]: Glandular Trichomes (GT) and Non-Glandular Trichomes (NGT) are localized at the surface; internal glands (IG) are found in the inner tissues of the mesophyll. These structures can adopt a myriad of sizes and shapes (long hairs, highly branched, etc.). There are mainly two types of GT: Capitate Glandular Trichomes (CGT) and Peltate Glandular Trichomes (PGT). These structures are mainly distinguished by their morphology (size and stalk length) and mode of secretion [7]. Terpenoids seem to predominate GT structures [8, 9]. IG are frequently present in the Rutaceae family, as for instance in *Citrus aurantium* leaves [10]. As for resin ducts, they are mainly present in the Pinaceae family [3].

It is thus important to consider the great variety of natural products and the complexity of their biosynthesis and storage processes within the plant kingdom but also within the plant itself. This implies that extraction techniques should take into account this complexity to improve extraction yield, selectivity and rate, and to ensure a targeted extraction of these secondary metabolites of great interest in food, pharmaceutical, nutraceutical and cosmetic industries [8, 11-13].

Extraction procedures range from conventional techniques (Soxhlet extraction, Clevenger extraction, maceration) to new “green” technologies such as the Ultrasound-Assisted Extraction (UAE). The positive contribution of power ultrasound (US) in solid-liquid extraction of natural products has been widely studied and proved throughout literature [14-19]. US-related performances gain consists of the amelioration of extraction yields, the acceleration of extraction kinetics as well as respecting the environment and providing extracts of higher quality [20-26]. Mechanisms behind UAE efficiency started to be unraveled allowing a better understanding of US-generated impacts. Erosion, sonoporation, shear forces, fragmentation, capillary effect and detexturation are the main reported mechanisms [27]. Those different mechanisms were generally observed individually, but a combination of these six mechanisms has been recently reported [28]. A special order was noticed and is presumed to be specific to the studied plant, and thus implying the necessity to further study the ultrasonic behavior in solid-liquid extraction according to the specificities of not only US but also plant matrices.

Within this objective, the present study aims to identify US impacts and mechanisms in the case of three plant species: bitter orange (*Citrus aurantium* L.), blackcurrant (*Ribes nigrum* L.) and artichoke (*Cynara scolymus* L.) leaves. UAE was compared to conventional procedure (silent). The surfaces of untreated and treated leaves were investigated by stereomicroscopic analysis and Scanning Electron Microscopy (SEM). Cyto-Histochemical study was carried out to study the spatial distribution of natural products (caffeic acid derivatives and flavonoids). US mechanisms, for each plant, were concluded on the basis of these different observations to point out differences/similarities according to plant structural properties.

2. Materials and methods

2.1.Plant material

Dry leaves of *Citrus aurantium* L. (bitter orange), *Ribes nigrum* L. (blackcurrant) and *Cynara scolymus* (artichoke) leaves were provided by Arkopharma (Carros, France). Leaves were collected in France in April 2018. They were dried at room temperature before being used without any prior pretreatment. Their initial moisture content ranged from 7.2 ± 0.4 % to 7.9± 0.6 %.

2.2. Localized sonication

To assess US-induced impacts on plant tissues, localized sonication was carried out using the system presented in supplementary material (figure S1). Leaves were individually submitted to the ultrasonic field emitted by an ultrasonic probe (1kW, UIP 1000 hdt, Hielscher Ultrasonics GmbH, Germany). In each experiment, the dry leaf was fixed in a perforated disk at 0.5 cm from the emitting probe. Localized sonication was performed at 20 kHz and 41.7±0.4 $W.cm^{-2}$. Two different US durations (30 and 60 min) were applied to follow the evolution of US-induced impacts over time. In all experiments, demineralized water was used as a solvent. Its temperature was maintained at 25±1°C with a cooling system connected to the double-jacket reactor. Conventional "silent" procedure (CV) was carried out using the same system without US for 60 min. Each experiment was carried out in triplicate.

2.3. Microscopic characterization procedures

2.3.1. Stereomicroscopic analysis

Studied leaves were analyzed before and after each treatment (initial, localized sonication, and CV procedure) using a Nikon AZ100 stereomicroscope (Nikon, Netherlands) equipped for fluorescence (excitation filter: 465-495 nm, emission filter: 515-555 nm) to reveal the presence of naturally fluorescent compounds. This stereomicroscopic investigation of leaves' surfaces aimed to identify their initial characteristic structures as well as the induced structural modifications/alterations. Leaves photos were taken at the same illumination conditions. All microscopic observations were done in triplicate.

2.3.2. Scanning Electron Microscopy (SEM)

Untreated and treated leaves were observed using a scanning electron microscope (XL30, FEI Philips, France). This microscopic investigation allowed the assessment of induced impacts on plant micro-structures depending on the extraction process. Contrarily to the stereomicroscopic analysis, SEM observations required a prior treatment of leaves' fragments which were fixed to a metal support and covered by a carbon adhesive (sputtering apparatus,

BD SCS 004, BALZERS) before analysis with SEM (7 Pa, 10 kV). Experiments were performed in triplicate.

2.3.3. Cyto-histochemistry

To better understand the complexity of plant internal tissues, it is crucial to carry out cyto-histochemical analysis of initial leaves. Tissues' preparation as well as tissues' sections and slides' preparation are detailed in supplementary material (figure S2). Samples were taken from each leaf and small fragments (5 to 7 mm) were instantly immersed into a fixative mixture (4 % paraformaldehyde, 4% glutaraldehyde and 1 % caffeic acid in a phosphate buffer 0.2 M) for 48h to preserve the integrity of plant tissues. Three rinsing cycles (3x1h) were then conducted to eliminate all fixative solution residues. Thereafter, samples were dehydrated in graded alcohol series (70 to 100%), infiltrated (24h) and embedded in resin (Technovit 7100, Kultzer). Once the resin has solidified, we proceeded to sections' cutting using a rotating microtome (Supercut 2065, Leica Microsystems, Germany). The obtained sections were then collected on microscope slides.

Regarding the staining step, two procedures were performed: (1) Neu's reagent revelation for all studied leaves and (2) Periodic acid-Schiff's reagent / Naphtol blue black reagent (PAS/NBB) in the case of artichoke leaf. Neu's reagent revelation aimed at investigating the spatial distribution of secondary metabolites such as flavonoids and caffeic acid derivatives using fluorescence. As for PAS/NBB reagent, it was used to point out structural similarities and /or differences between PGT of both adaxial and abaxial surfaces of artichoke leaf. Neu's reagent solution was prepared as described by Andary et al. [29]. As regards PAS/NBB reagent, it was prepared following procedure described by El Maâtaoui and Pichot [30].

All observations were performed using Leica DMR microscope equipped with dark field, bright field, phase contrast and UV-illumination (Leica DMR, Leica Microsystems, Germany; excitation filter: 340-380 nm, emission: 425 nm). Sections stained with Neu's reagent were analyzed using an excitation filter of 340-380 nm and an emission filter at 425 nm. Under these operating conditions, leaf tissues emit different fluorescence depending on their phenolic content. Flavonoids are revealed in greenish-yellow. Caffeic acid derivatives are light blue [29].

For PAS/NBB, stained sections were analyzed using phase contrast. PAS/NBB reagent has the ability to reveal polysaccharides in pink color and proteins in dark blue. All experiments were performed in triplicate.

3. Results and Discussion

3.1. Process-induced impacts depending on plant structures

Bitter orange, blackcurrant and artichoke leaves were analyzed with SEM and stereomicroscope to identify their main secondary metabolites' containing structures and to evaluate process-related structural modifications. CV and US treatments were conducted as described in section 2.2. Investigations of these three leaves, before and after each treatment, will be presented and discussed in the following sections.

3.1.1. Bitter orange leaf (*C. aurantium*)

As presented is figure 1, the presence of large internal glands (IG) is the major property of bitter orange leaf. Those specialized structures are highly present on the adaxial surface [figures 1.1 (a,b)] as previously described in many studies [31,32]. Stereomicroscopic investigation, presented in figure 1.1.c, highlighted the abundance of highly fluorescent natural compounds emanating from the whole adaxial surface. However, IG seemed to not emit any natural fluorescence. Their secondary metabolites are presumably stored deeper in their storage cavities embedded in the inner tissues of the mesophyll.

Regarding the process-induced impacts, the leaf adaxial surface appeared to be intact after 60 min of CV procedure. As shown in figure 1.2.d and 1.2.e, adaxial cuticle and IG were undamaged [compare figure 1.2 (d,e) with figure 1.1(a,b)]. In contrast, US treatment impacted significantly the adaxial surface by inducing ruptures into the cuticle which gives access to the underlying tissues (see figure 1.3.g). Moreover, large openings were noticed in the case of IG (figure 1.3.h) which is supposed to promote solvent penetration and solubilization of their secondary metabolites. Along with these observations, fluorescence intensity has dramatically decreased after US application during 60 min compared to that of both initial leaf and leaf submitted to the CV procedure (compare figure 1.3.i with figures 1.1.c and 1.2.f).

These observations showed that 60 minutes under US impacted bitter orange leaf by two different mechanisms according to plant structures: (1) sonoporation in the case of IG and (2) fragmentation in the case of the cuticle. It is worth mentioning that sonoporation started at thirty minutes of US treatment with relatively small openings into the IG envelopes (see figure 2.2). Larger openings were then generated resulting in their total explosion at sixty minutes of localized sonication (see figure 2.3). As for fragmentation mechanism, it was firstly observed after 60 min of US application.

Similar mechanical effects were previously noticed in plant solid/liquid extraction field in the case of rosemary leaf as a part of our previous work [28]. As described in this article, US-

generated pores were firstly identified at 20 min of US application. US-induced fragmentation has also been reported in the same study at 30 min of US treatment.

Therefore, US could impact different plant species through the same mechanisms such as sonoporation and fragmentation. However, from a temporal point of view, US-induced structural changes could take completely different pathways.

3.1.2. Blackcurrant leaf (*R. nigrum*)

SEM and stereomicroscopic investigations of blackcurrant leaf' abaxial surface are presented in figure 3. The main characteristics of this leaf are the presence of external PGT and NGT (see figures 3.1.a and 3.1.b) as previously shown by Kerslake [7]. We can notice that PGT are more abundant than NGT which are mainly located in the midrib. Moreover, PGT appeared to be the most fluorescent structures of leaf abaxial surface (see figure 3.1.c) suggesting a high presence of naturally fluorescent compounds in those external specialized structures.

Regarding the process-related impacts, CV procedure appeared to preserve those two characteristic structures as well as the integrity of the cuticle (see figures 3.2.e and 3.2.f). As shown in figure 3.2.e, after 60 min of CV treatment, PGT have the same aspect as that of the initial leaf (balloon-shape, intact envelope, etc.). This is also the case for the long NGT which seemed to be preserved (figure 3.2.f). Those observations are in agreement with the fluorescence intensity which remained stable after 60 min of CV procedure (compare figure 3.2.g with figure 3.1.c).

However, focusing our attention on the localized sonication, many induced impacts can be identified (figure 3.3). Starting with the leaf surface, it can be noticed that the cuticle seemed to be shrunk and dehydrated (figure 3.3.i). In addition, PGT were completely exploded after 60 min of US application giving access to their storage cavities' content and their secretory cells (see figure 3.3.i). Surprisingly, NGT were more resistant to the ultrasonic field (see figure 3.3.j). Most of those structures were undamaged after 60 min; only some NGT were eroded (figure 3.3.j) which provides access to the secondary metabolites of the underlying tissues.

Stereomicroscopic observations provided an excellent comparison between the CV procedure and the localized sonication (compare figure 3.2.g with figure 3.3.k). As shown in these figures, within the same leaf, the left side was submitted to the CV procedure for 60 min (figure 3.2.g) while the right side was submitted to the ultrasonic field for the same duration (figure 3.3.k). It is clear that, contrarily to the CV procedure, US application generated different physical impacts on abaxial leaf surface [compare figure 3.2 (g,h) with figure 3.3 (k,l)]. The major noticed impacts are large ruptures into the cuticle and the explosion of PGT

(see figures 3.3.k and 3.3.l). A drastic decrease in fluorescence intensity has also been noticed indicating the decrease in the concentration of naturally fluorescent compounds.

Regarding the evolution of the induced impacts during US application (figure 4), it can be noticed that the generated damage in PGT started at 30 min of US treatment with small openings into their smooth envelope (figure 4.2.c). Their total explosion was observed at 60 min of US application (figure 4.3.e). However, 30 min of US application did not induce any impact on NGT (figure 4.2.d), further confirming their particular resistance.

To summarize, blackcurrant leaves' PGT and NGT are both located in the surface; whereas they had not the same resistance level to the ultrasonic field. These observations pointed to the strong probability that those two external structures have different structural constitutions. Hence, US efficiency can be limited by the resistance of some specialized structures such as in the case of NGT of blackcurrant leaf.

Our results showed that US impacted blackcurrant abaxial leaf surface by three different mechanisms: (1) sonoporation resulting in the explosion of PGT, (2) fragmentation mechanism implying large fractures into the cuticular layer and (3) erosion of some NGT. The first mechanism noticed was the sonoporation starting at 30 min. The fragmentation mechanism was observed at 60 min. However, NGT' erosion mechanism appeared to require longer US treatments since it began at 60 min. It is important to note that the erosion mechanism has already been reported in many studies [23, 33, 34]. It was also recently identified in our previous work in the case of rosemary leaf [28]. An absolutely crucial point to mention is that, in the case of rosemary leaf, mechanical erosion of NGT was observed after only 5 min of US application. Total abrasion of those long and branched NGT was noticed after 20 min contrarily to our current observations of blackcurrant leaves' NGT. Moreover, bitter orange leaves' IG, embedded into the internal tissues, had the same behavior as that of blackcurrant leaves' external PGT (see section 3.1.1) which implies the crucial importance of the containing' structures constitution. These different observations proved that US-induced impacts are strongly dependent on plant families and their different characteristic structures.

3.1.3. Artichoke leaf (*C. scolymus*)

Observations concerning artichoke initial leaf are presented in figure 5. SEM analyses pointed to the likelihood between the specialized structures present in both adaxial and abaxial surfaces which are PGT and NGT [compare figure 5.1(a,b) with figure 5.2 (d,e)]. It is noteworthy that NGT are more abundant on abaxial surface where they cover densely the whole surface (compare figure 5.1.b with figure 5.2.e). PGT of both surfaces are balloon-

shaped; those of abaxial surface are hidden by the massive presence of NGT. These observations are in accordance with those of Brutti et al [35].

Stereomicroscopic analysis pointed to a higher fluorescence of abaxial surface compared to that of the adaxial surface (compare figure 5.1.c with figure 5.2.f). This important fluorescence could be related to the massive presence of PGT which are proved to be the most naturally fluorescent structures of artichoke leaf (figure 5.2.f).

Figure 6 shows process-related impacts on adaxial leaf surface. As seen in this figure, having undergone CV procedure (figure 6.2), adaxial leaf structures were entirely preserved: intact balloon-shaped PGT and long NGT. However, stereomicroscopic observations revealed a slight decrease in fluorescence intensity (compare figure 6.2.h with figure 6.1.d) which could be explained by the diffusion of hydrophilic natural compounds to the surrounding solvent. As regards the localized sonication (figure 6.3), induced impacts were more extensive. Considering SEM investigation, it can be seen that US treatment resulted in pronounced damage into the adaxial cuticle (figure 6.3.i). Many large fractures and holes were noticed, thus enhancing the accessibility to the inner tissues. NGT were also impacted after 60 min of US application. As shown in figure 6.3.j, most of NGT were eroded promoting the liberation of their content into the surrounding solvent as well as solvent penetration into the underlying tissues. Interestingly, PGT were more resistant to the ultrasonic field (figure 6.3.j). Only some slight deformations into their envelopes could be noticed. Hence, longer US treatment durations seemed to be required to reach the total explosion of those structures. Consequently, there is evidence to suggest the hypothesis that PGT envelopes have a different constitution compared to that of the cuticle and NGT, thus explaining their resistance to the ultrasonic treatment. These different SEM observations were confirmed by stereomicroscopic analyses showing a noticeable decrease in fluorescence intensity of the adaxial cuticle. In contrast, PGT have retained their natural fluorescence [compare figure 6.3 (k,l) with figure 6.1 (c,d)].

To summarize, US impacted artichoke leaf adaxial surface by three different mechanisms: (1) fragmentation in the case of adaxial cuticular layer (ruptures and large holes), (2) shear forces inducing deformations into adaxial PGT' envelopes and (3) erosion of NGT.

Investigation of the abaxial leaf surface investigation is presented in figure 7. It can be noted that CV procedure had not impacted leaf structures [compare figure 7.2 (e,f) with figure 7.1 (a,b)]. Long NGT were preserved; they covered densely the entire abaxial surface. PGT were also undamaged [see figure 7.2 (e,f)]. These observations are in coherence with stereomicroscopic investigation revealing constant fluorescence intensity compared to that of initial leaf abaxial surface [compare figure 7.2 (g,h) with figure 7.1 (c,d)].

Regarding the localized sonication (figure 7.3), abaxial cuticle was extremely damaged: large fractures and holes were observed. NGT were also impacted; most of them were completely exfoliated (figure 7.3.i). Surprisingly, abaxial PGT were highly impacted; most of them were completely exploded (figure 7.3.j) giving access to their secretory cells. Along with these SEM observations, general fluorescence level has significantly dropped (compare figure 7.3 (k,l) with figure 7.1 (c,d)).

In the case of abaxial surface, US acts through four different mechanisms: (1) fragmentation in the case of abaxial cuticular layer (large fractures), (2) shear forces and (3) sonoporation inducing respectively deformations and pores into abaxial PGT' envelopes and (4) erosion of abaxial NGT. Figure 8 illustrates the gradual induced impacts during US treatment of both adaxial and abaxial surfaces. This figure further outlines differences between adaxial and abaxial PGT behaviors during US treatment. Indeed, thirty minutes of US application induced some deformations into the adaxial PGT' envelopes (compare figure 8.2.c with figure 8.1.a). These induced deformations are presumably related to shear forces generated by the ultrasonic wave propagation into the liquid solvent [28]. Surprisingly, adaxial PGT having undergone 60 min of US application maintained the same shape and aspect as that after 30 min of US application (compare figure 8.3.e and figure 8.2.c). Therefore, 60 min under US-generated shear forces were insufficient to break-down their apparently resistant envelopes. In the case of abaxial PGT, shear forces-related deformations appeared also at 30 min (figure 8.2.d). Total explosion of those structures was noticed at 60 min of US application (figure 8.3.f).

These observations suggest that adaxial and abaxial PGT' envelopes have different constitutions. Cyto-chemical investigation was carried out to assess this hypothesis. Microscopic observations of adaxial and abaxial PGT sections after staining with PAS/NBB reagents are presented is figure 9. It is apparent from this figure that adaxial and abaxial PGT have the same chemical constitution (compare figure 9.a with figure 9.b). Proteins appeared to be highly concentrated in the secretory cells stained in dark blue. As regards polysachharides, they are mainly located in the inner part of the secretory cavity envelope revealed in pink color.

In contrast, from a structural standpoint, adaxial PGT envelope seemed to be thicker than that of abaxial PGT (compare figure 9.b with figure 9.a). It is worth remembering that abaxial PGT are hidden and thus protected by the massive presence of abaxial NGT contrarily to adaxial PGT which are directly exposed to the biotic and abiotic conditions (temperature, UV-

light, external attacks, etc.). Thus, the thickening of adaxial PGT envelopes could represent a means of protection against all external disturbances.

Combining these results with SEM and stereomicroscopic observations, it can be seen that thickness of adaxial PGT plays a key role in their particular resistance to the ultrasonic action.

3.2.Cyto-histochemistry as a decision tool for a targeted extraction

The section 3.1 was devoted to the understanding of US-induced impacts depending on plant families/species and plant structures. It proved the importance of SEM and stereomicroscopic plant analyses allowing the investigation of their characteristic structures as well as their resistance level to the ultrasonic field. However, those two microscopic techniques (SEM and stereomicroscopic) provide specific information limited to the surface structures such as external specialized structures and the cuticular layer.

For example, in the case of bitter orange leaf IG, SEM and stereomicroscopic investigation provided important insights into the explosion of those structures (see section 3.1.1). However, there is no evidence that US application allowed the extraction of their storage cavity' and secretory cells' contents. Further analyses are then required to better localize plant secondary metabolites and to assess US efficiency. For such a purpose, cyto-histochemical investigation was performed to better understand the spatial distribution of plant secondary metabolites.

Figure 10 shows bitter orange, blackcurrant and artichoke leaves' sections after staining with Neu's reagent. As seen in this figure, for the three studied species, leaf tissues emitted two different fluorescence colors depending on their phenolic contents: a greenish-yellow color for flavonoids and a light blue in the case of caffeic acid derivatives. Microscopic observations pointed out that the three studied leaves are highly rich in flavonoids and caffeic acid derivatives. However, it is important to note that secondary metabolites' spatial distribution is different depending on plant species and structures (figure 10). In the case of bitter orange leaf (figure 10.a), caffeic acid derivatives are present in the cuticular layer highly stained in light blue. As for flavonoids, revealed in greenish-yellow, they are located deeper in the inner tissues (mesophyll tissues and IG' secretory cells) (see figure 10.a).

Blackcurrant leaf is also rich in caffeic acid derivatives (see figure 10.b). Those compounds are mainly identified in adaxial and abaxial cuticular layers. As regards flavonoids, they are present in the external PGT (secretory cells and envelopes). Inner tissues (epidermal cells and mesophyll tissues) were highly stained in yellowish-green indicating their high concentration in flavonoids (figure 10.b). Concerning artichoke leaf (figure 10.c), flavonoids appeared to be present in the entire leaf' external (NGT and PGT) and inner tissues (epidermal cells and mesophyll' inner tissues). Overall, plant cyto-histochemical investigation could represent a

means to determine the spatial distribution of active natural compounds such as flavonoids and caffeic acid derivatives and thus merits further attention.

4. Conclusion and persepectives

Our microscopic observations proved the complexity of plant structures. A heterogeneous spatial distribution of secondary metabolites (caffeic acid derivatives and flavonoids) and a diversity of their containing structures were noticed. The three studied plant species (bitter orange, blackcurrant and artichoke leaves) evolve different structural properties and different specialized storage structures. IG are the main characteristic of bitter orange adaxial surface. NGT and PGT are present in blackcurrant abaxial leaf surface. As for artichoke leaf, NGT and PGT are highly abundant in both abaxial and adaxial leaf surfaces.

Contrarily to the CV procedure which preserves plant structures, US application generated several structural alterations especially on specialized structures. However, US-related impacts are strongly dependent on plant species. In the case of bitter orange leaf, IG were completely damaged after 60 min of US treatment. Adaxial cuticle was also highly impacted. Therefore, in the case of bitter orange leaf, US acts through two different mechanisms: (1) sonoporation in the case of IG and (2) fragmentation in the case of adaxial cuticle. Three mechanisms were observed in the case of blackcurrant leaf: (1) sonoporation implying the explosion of PGT, (2) fragmentation of the abaxial cuticular layer and (3) erosion of NGT. The study of artichoke further proved the complexity of plant matrices and the considerable differences observed between their two surfaces (abaxial vs adaxial). Indeed, US impacted the artichoke leaf surfaces through different mechanisms. Three mechanisms were noticed in the case of adaxial surface: (1) Fragmentation pf the cuticular layer, (2) shear forces on the PGT and (3) erosion of NGT. For the abaxial surface, four mechanisms were observed: (1) fragmentation of the cuticle, (2) shear forces and (3) sonoporation on PGT, and (4) erosion of NGT. This implies that adaxial and abaxial PGT have not the same resistance level which confirms the complexity of plant structures behavior while being submitted to the ultrasonic field.

Moreover, this study could be a valuable tool for assessing UAE performances. As an example, cyto-histochemical study of bitter orange leaf before and after treatment (CV treatment vs UAE) was carried out and presented in figure 11. Considering the CV procedure, orange bitter leaf exhibits the same structural properties compared to the initial structural properties (compare figure 11.b with figure 11.a). The cuticular layer was undamaged. Plant cells appeared to maintain their morphological integrity. In contrast, a noticeable decrease in

fluorescence intensity has been observed (compare figure 11.b with figure 11.a). Light blue fluorescence of the adaxial cuticular layer had dropped dramatically compared to that of the initial leaf. In the same way, the greenish-yellow fluorescence of the inner tissues has decreased significantly. These two observations could be related to the diffusion of hydrophilic caffeic acid derivatives and flavonoids to the extraction solvent. Regarding UAE, many structural alterations can be noticed. Starting with the cuticular layer, many deep fractures were identified. Moreover, significant damage has been noticed in the inner cells compared to those of the initial leaf and leaf after CV procedure (compare figure 11.c with figure 11.a and figure 11.b). This noticeable damage includes cells shrinkage, vacuole regression and cell wall lysis (see figure 11.c). Together, these US-induced alterations enhance solvent penetration into inner tissues as well as the release of secondary metabolites. This results in a dramatic decrease in greenish-yellow and light blue fluorescence after 60 min of UAE, indicating an efficient extraction of flavonoids and caffeic acid derivatives of bitter orange leaf.

Based on our findings, spatial distribution and temporal extraction of secondary metabolites and the comprehension of plant structural properties should be considered as a decision tool for a targeted UAE which could take completely different pathways according to plant species and their structural resistance level. It became important to start with microscopic analysis before proceeding with US procedure on an unknown or non-studied plant. This breakthrough opens the door to quick and easy methods for localizing glands and structures containing bioactive compounds but also US energy and time required for detexturation. The decision tool will also permit to target specific secondary or primary metabolites providing thus a complete and selective extraction.

References

[1] K.H. Neumann, A. Kumar, J. Imani. Secondary metabolism, chapter 10, in: K.H. Neumann, A. Kumar, J. Imani. Plant Cell and Tissue Culture-A Tool in Biotechnology Basics and Application, 2009 Springer-Verlag Berlin Heidelberg, 2009, pp 181-225.

[2] A. Tissier, J.A. Morgan, N. Dudareva. Plant Volatiles: Going 'In' but not 'Out' of Trichome Cavities. Trends in Plant Science. 22 (2017) 931-938.

[3] F. Fahn, Structure and Function of Secretory Cells, chapter 2, in: D.L. Hallahan and J.C Gray, Advances in botanical research incorporating advances in plant pathology Plant trichomes, Academic press, 2000, pp 36-75.

[4] Verpoorte R (2000) Secondary metabolism. In: Verpoorte R, Alfermann AW (eds) Metabolic engineering of plant secondary metabolism. Kluwer Academic, Dordrecht, pp 1–29.

[5] E. Werker. Trichome Diversity and Development, chapter 1, in: D.L. Hallahan and J.C Gray, Advances in botanical research incorporating advances in plant pathology Plant trichomes, Academic press,2000, pp 1-35.

[6] A. Tissier. Plant secretory structures: more than just reaction bags. Current Opinion in Biotechnology.49 (2018) 73–79.

[7] D.L. Hallahan, Monoterpenoid Biosynthesis in Glandular Trichomes of Labiate Plants, chapter 3, in: D.L. Hallahan and J.C Gray, Advances in botanical research incorporating advances in plant pathology Plant trichomes, Academic press, 2000, pp 76-120.

[8] S.O. Duke, C. Canel, A.M. Rimando, M.R. Tellez, M.V. Duke, R.N. Paul. Current and Potential Exploitation of plant glandular trichome productivity, chapter 4, in: in: D.L. Hallahan and J.C Gray, Advances in botanical research incorporating advances in plant pathology Plant trichomes, Academic press, 2000, pp 121-151.

[9] P. Baran, K. Aktaş, C. Özdemir. Structural investigation of the glandular trichomes of endemic. *Salvia smyrnea* L. South African Journal of Botany 76 (2010) 572–578.

[10] G.W. TURNER. A Brief History of the Lysigenous Gland Hypothesis. The botanical review. 65 (1999) 76-88.

[11] H.P.S. Makkar, P. Siddhuraju, K. Becker. Plant Secondary Metabolites. Humana Press Inc, Totowa, New Jersey, 2007, pp 1-130.

[12] A. Bernhoft. A brief review on bioactive compounds in plants. Proceedings from a Symposium held atThe Norwegian Academy of Science and Letters, Oslo, Norway, 2010.

[13] F. Chemat, N. Rombaut, A.-S. Fabiano-Tixier, J.T. Pierson, A. Bily, Green extraction: from concepts to research, education, and economical opportunities, Chapter 1, in: F. Chemat, J. Strube (Eds.), Green Extraction of Natural Products: Theory and Practice, Wiley CH, 2015, pp. 1–36.

[14] F.J. Barba, C.M. Galanakis, M.J. Esteve, A. Frigola, E. Vorobiev. Potential use of pulsed electric technologies and ultrasounds to improve the recovery of high-added value compounds from blackberries. Journal of Food Engineering 167 (2015) 38–44.

[15] M. Koubaa, H. Mhemdi, F.J. Barba, S. Roohinejad, R. Greiner, E. Vorobiev. Oilseed treatment by ultrasounds and microwaves to improve oil yield and quality: An overview. Food Research International. 85 (2016) 59–66.

[16] M. Koubaa, F.J. Barba, N. Grimi, H. Mhemdi, W. Koubaa, N. Boussetta, E. Vorobiev. Recovery of colorants fromred prickly pear peels and pulps enhanced by pulsed electric field and ultrasound. Innovative Food Science and Emerging Technologies 37 (2016) 336–344.

[17] N.N. Misra, M. Koubaa, S. Roohinejad, P. Juliano, H.Alpas, Rita S. Inácio, J.A. Saraiva, F.J. Barba. Landmarks in the historical development of twenty first century food processing technologies. Food Research International 97 (2017) 318–339.

[18] T. Jiang, S. Zhan, S. Li, Z. Zhu, J. He, J.M. Lorenzo and F.J Barbac. From ‘green’ technologies to ‘red’ antioxidant compounds extraction of purple corn: a combined ultrasound–ultrafiltration– purification approach. J Sci Food Agric 98 (2018) 4919–4927.

[19] M. Marić, A.N Grassinob, Z. Zhuc, F.J. Barbad, M. Brnčić, S.R. Brnčić. An overview of the traditional and innovative approaches for pectin extraction from plant food wastes and by-products: Ultrasound-, microwaves-, and enzyme-assisted extraction. Trends in Food Science & Technology 76 (2018) 28–37.

[20] M. Virot, V. Tomao, C. Le Bourvellec, C.M.C.G. Renard, F. Chemat. Towards the industrial production of antioxidants from food processing by-products with ultrasound-assisted extraction Ultrasonics Sonchemistry. 17 (2010) 1066-1074.

[21] T. J. Mason, F. Chemat, M. Vinatoru. The Extraction of Natural Products using Ultrasound or Microwaves. Current organic chemistry. 15 (2011) 237-247.

[22] S. Périno-Issartier, C. Ginies, G. Cravotto, F. Chemat. A comparison of essential oils obtained from lavandin via different extraction processes: Ultrasound, microwave, turbohydrodistillation, steam and hydrodistillation. Journal of Chromatography A. 1305 (2013) 41-47.

[23] S. Both, F. Chemat, J. Strube. Extraction of polyphenols from black tea - Conventional and ultrasound assisted extraction. Ultrasonics Sonochemistry. 21 (2014), 21 (3) 1030-1034.

[24] I.Majid, G.A. Nayik, V. Nanda. Ultrasonication and food technology: A review. Cogent Food & Agriculture.1 (2015) 107-122.

[25] A-G. Sicaire, M.A Vian, F. Fine, P. Carré, S. Tostain, F. Chemat. Ultrasound induced green solvent extraction of oil from oleaginous seeds. Ultrasonics Sonochemistry. 31 (2016) 319-329.

[26] L. Paniwnyk. Applications of ultrasound in processing of liquid foods: A review. 38 (2017) 794-806.

[27] F. Chemat, N. Rombaut, A-G. Sicaire, A. Meullemiestre, A-S. Fabiano-Tixier, M. Abert-Vian. Ultrasound assisted extraction of food and natural products. Mechanisms, techniques, combinations, protocols and applications. A review. Ultrasonics Sonochemistry. 34 (2017) 540-560.

[28] B. Khadhraoui, M. Turk, A.S. Fabiano-Tixier, E. Petitcolas, P. Robinet, R. Imbert, M. El Maâtaoui, F. Chemat. Ultrasonics Sonochemistry. 42 (2018) 482–492.

[29] C. Andary, L. Mondolot-Cosson, G.H. Dai, In situ detection of polyphenols in plant micro-organism interactions, in: M. Nicole, V. Gianinazzi-Pearson (Eds.), Histology, Ultrastructure and Molecular Cytology of Plant-Microorganism Interactions, Kluwer Academic Publishers, Netherlands, 1996, pp. 43–53.

[30] Mohamed El Maâtaoui1, Christian Pichot. Planta. (1999) 208: 345-351.

[31] K. Periyanayagam, S. Dhanalakshmi, V. Karthikeyan. Pharmacognostical, SEM and EDAX profile of the leaves of *Citrus aurantium* L. (Rutaceae). Innovare Journal of Health Sciences.1 (2013) 1-5.

[32] F. Raimondo, P.Trifilò, M.A. Lo Gullo. Does citrus leaf miner impair hydraulics and fitness of citrus host plants? Tree Physiology. 33 (2013) 1320-1327.

[33] M. Degrois, D. Gallant, P. Baldo, A. Guilbot. The effects of ultrasound on starch grains. Ultrasonics. (1974) 129-132.

[34] L. Petigny, S. Périno-Issartier, J. Wajsman, F. Chemat. Batch and Continuous Ultrasound Assisted Extraction of Boldo Leaves (Peumusboldus Mol.). Int. J. Mol. Sci. 14 (2013) 5750-5764.

[35] C.B. Brutti, E.J. Rubio, B.E. Llorente, N.M. Apostolo. Artichoke leaf morphology and surface features in different micropropagation stages. Biologia Platarum. 45 (2002) 197-204.

List of figures

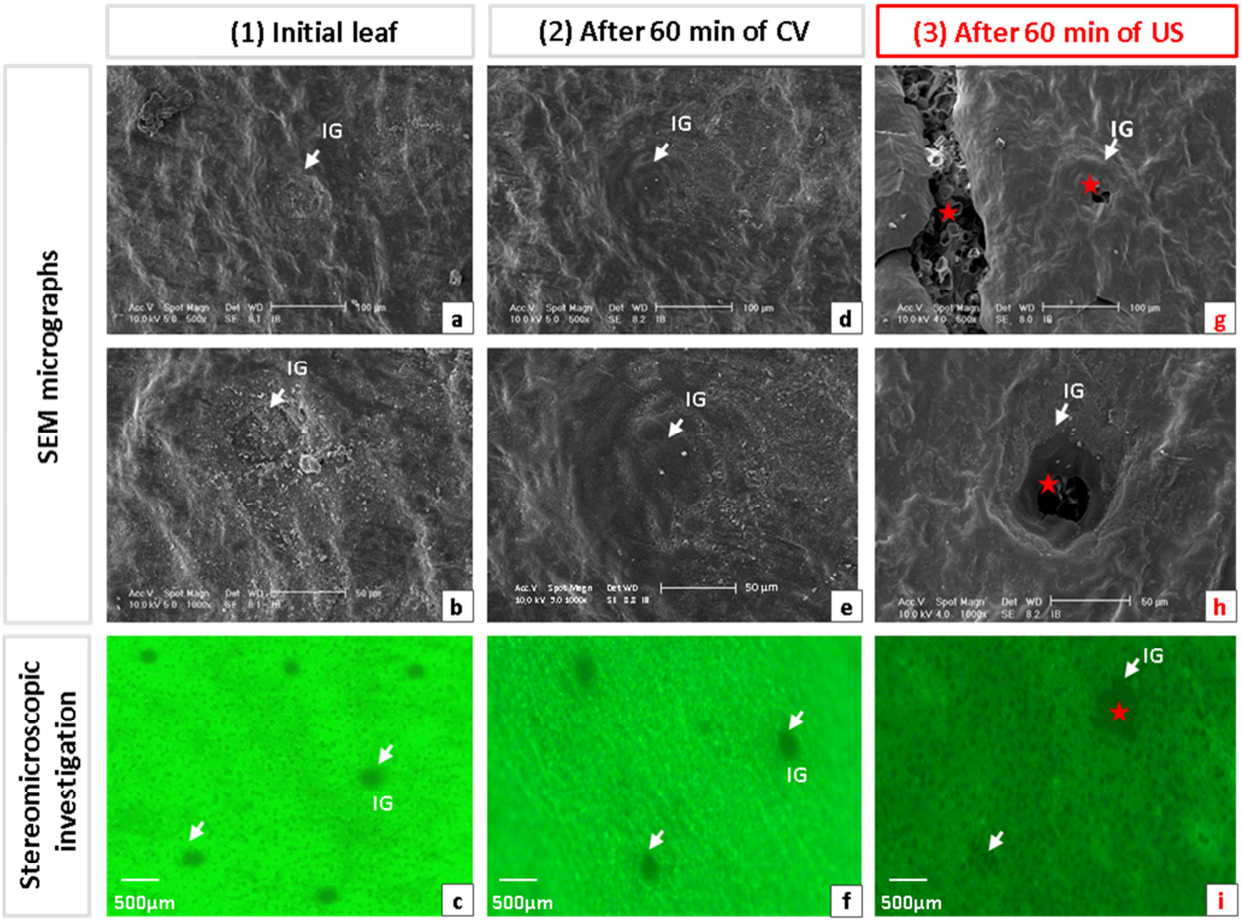

Figure 1. Investigation of *C. aurantium* adaxial leaf surface.

(1) Investigation of the initial leaf: SEM micrographs (a-b) and stereomicroscopic investigation under UV-illumination (c). (2) Leaf investigation after 60 min of CV procedure: SEM micrographs (d-e) and stereomicroscopic investigation under UV-illumination (f). (3) Leaf Investigation after 60 min of US treatment: SEM micrographs (g-h) and stereomicroscopic investigation under UV-illumination (i).

IG: Internal Gland; ★ : rupture/opening zone.

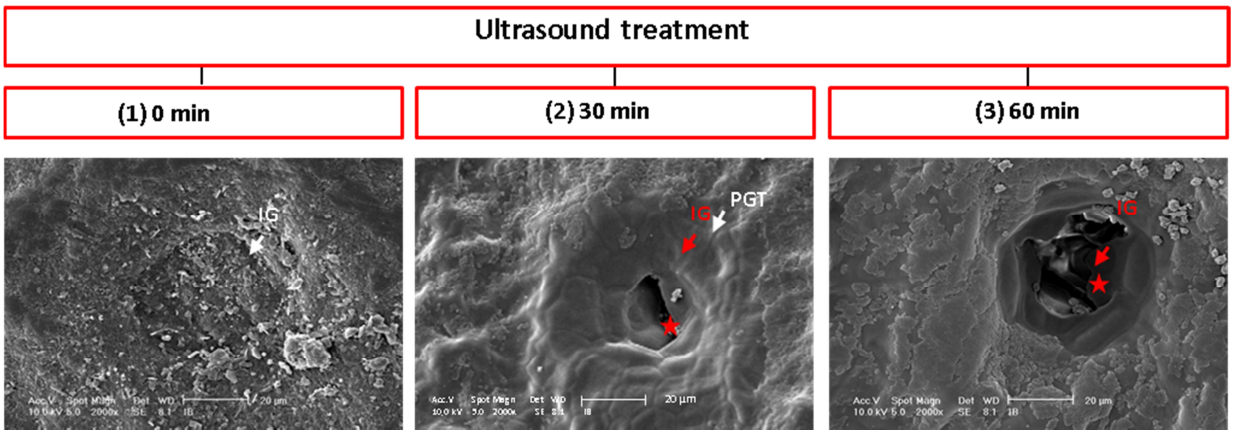

Figure 2. SEM micrographs of *C. aurantium* adaxial leaf surface during US treatment. (1) Initial leaf. (2) After 30 min of US treatment. (3) After 60 min of US treatment. IG: Internal Gland; ★ : rupture/opening zone.

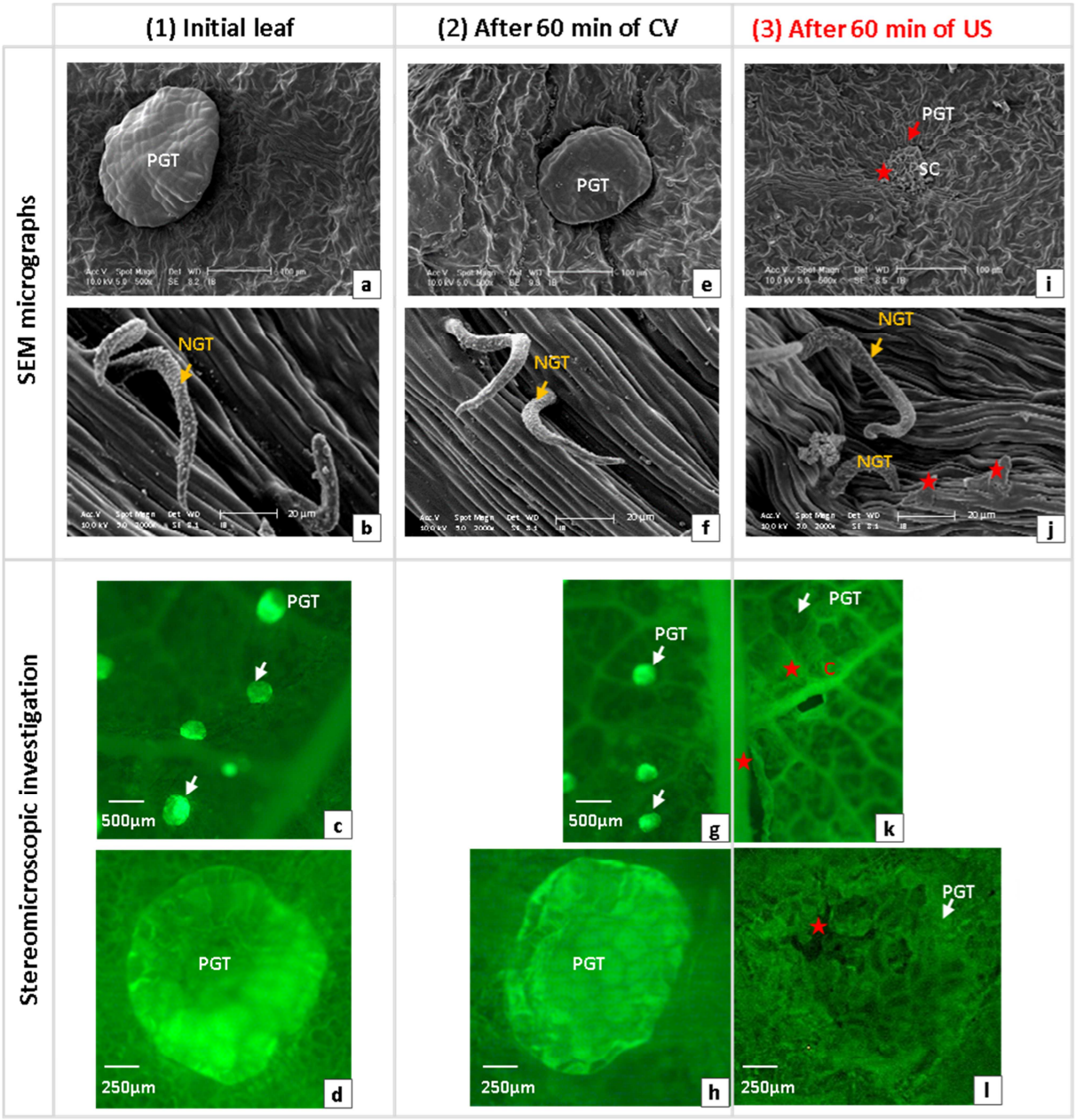

564

565 **Figure 3.** Investigation of *R. nigrum* abaxial leaf surface.

566 (1) Investigation of the initial leaf: SEM micrographs (a-b) and stereomicroscopic investigation under
567 UV-illumination (c-d). (2) Leaf Investigation after 60 min of CV procedure: SEM micrographs (e-f)
568 and stereomicroscopic investigation under UV-illumination (g-h). (3) Leaf Investigation after 60 min
569 of US treatment: SEM micrographs (i-j) and stereomicroscopic investigation under UV-illumination
570 (k-l).

571 PGT: Peltate Glandular Trichomes; SC: Secretory Cells; C: abaxial Cuticle; ★ : rupture/ opening zone.

572

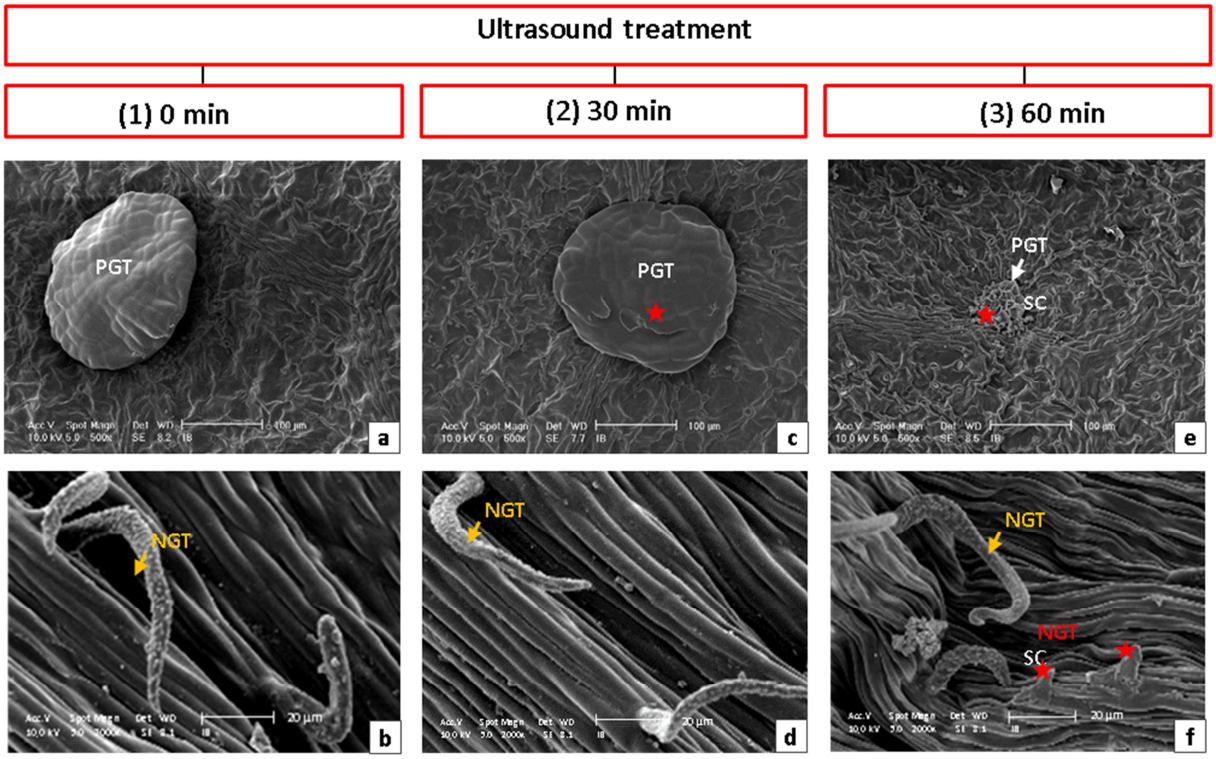

Figure 4. SEM micrographs of PGT and NGT of the *R. nigrum* abaxial leaf surface during US treatment. (1) Investigation of the intial leaf: PGT (a) and NGT (b). (2) Leaf investigation after 30 min of US treatment: PGT (c) and NGT (d). (3) Leaf investigation after 60 min of US treatment: PGT (e) and NGT (f).

PGT: Peltate Glandular Trichomes; NGT: Non-Glandular Trichomes; SC: Secretory Cells; ★ : rupture/opening zone.

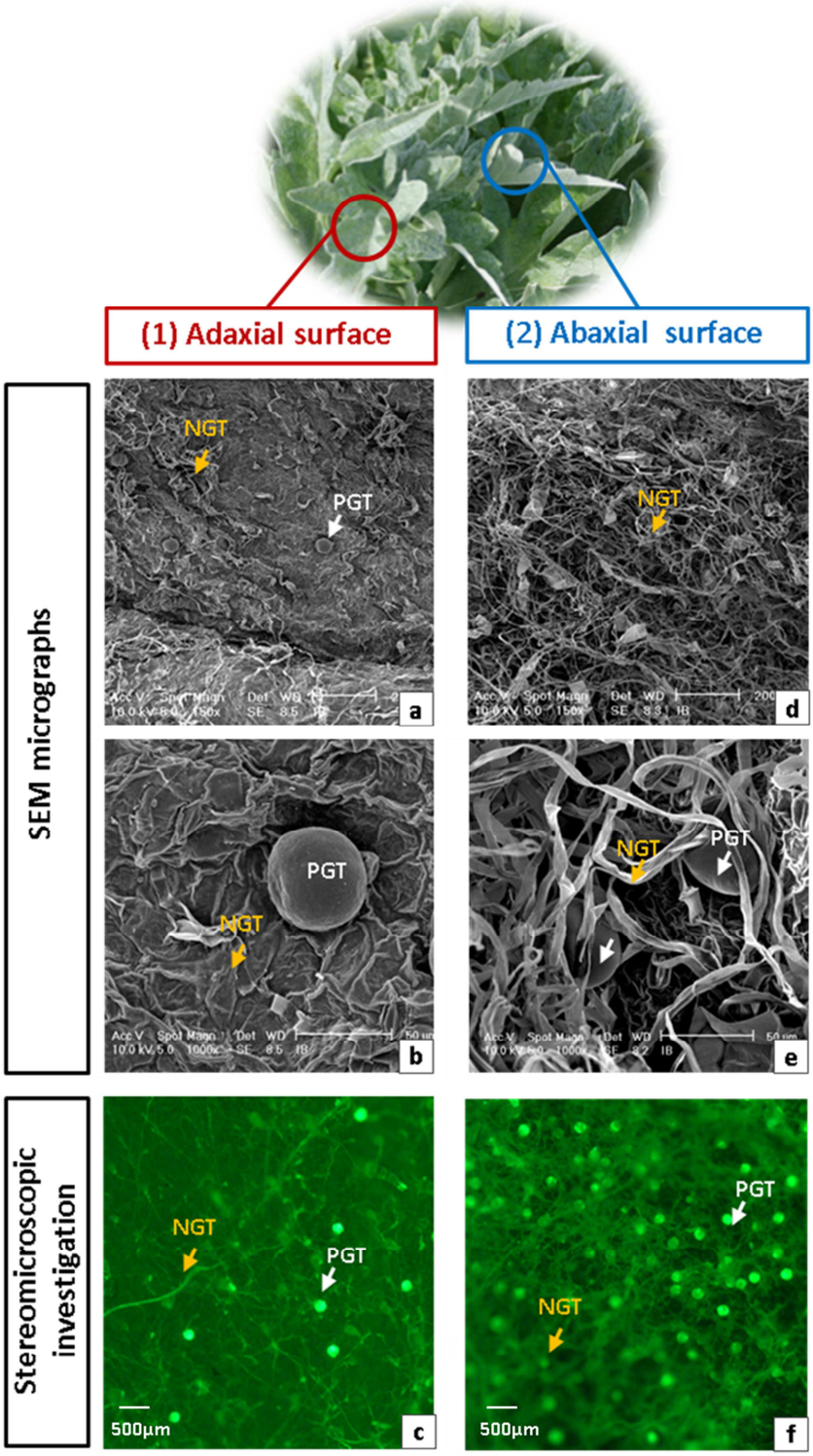

583

584 **Figure 5.** Investigation of *C. scolymus* adaxial and abaxial surfaces.

585 Adaxial surface: SEM micrographs (a-b) and stereomicroscopic investigation (c). (2) Abaxial surface:

586 SEM micrographs (d-e) and stereomicroscopic investigation (f).

587 PGT: Peltate Glandular Trichomes; NGT:Non-Glandular Trichomes.

588

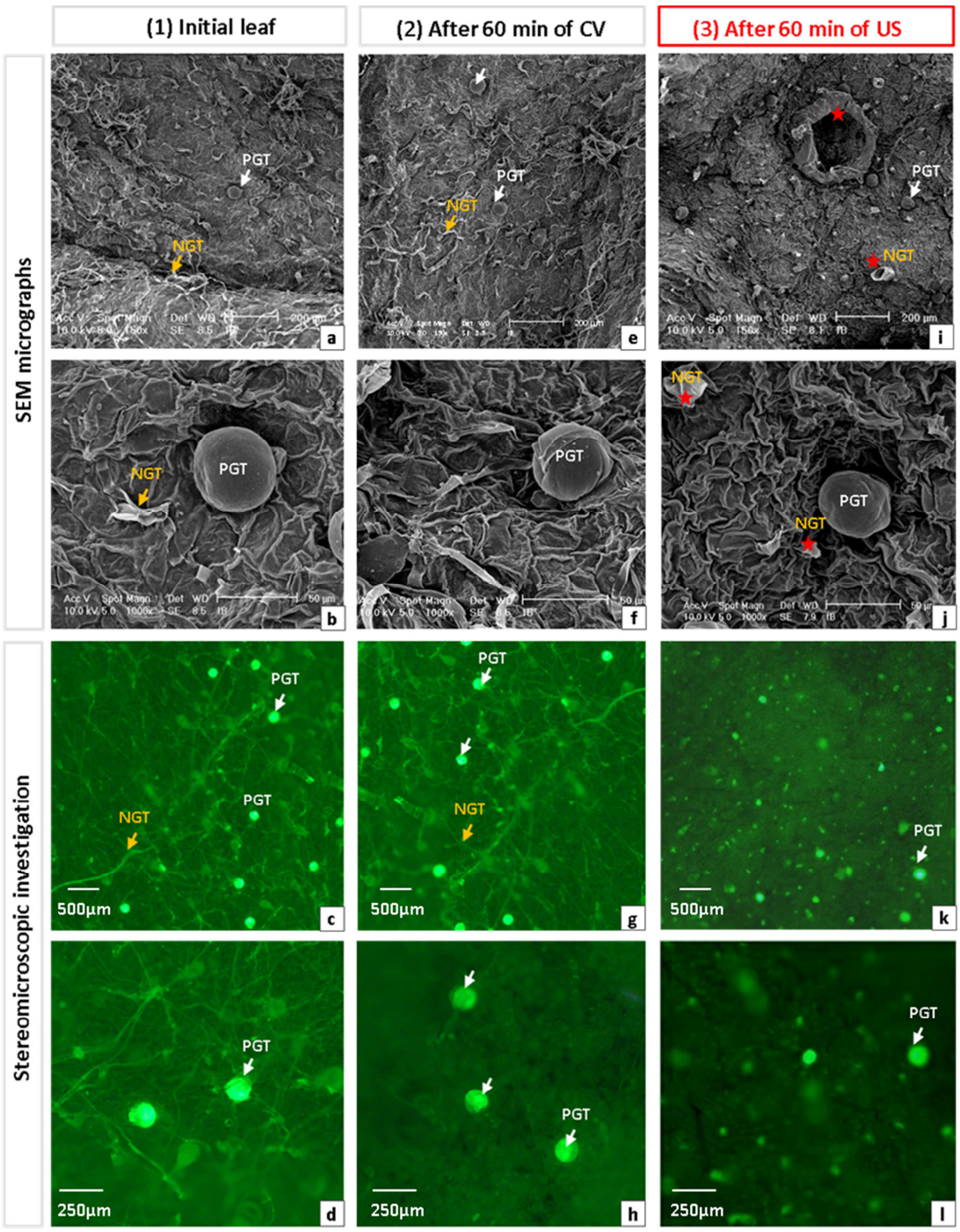

589

590 **Figure 6.** Investigation of *C. scolymus* adaxial leaf surface. (1) Investigation of the initial leaf: SEM
591 micrographs (a-b) and stereomicroscopic investigation under UV-illumination (c-d). (2) Leaf Investigation after
592 60 min of CV procedure: SEM micrographs (e-f) and stereomicroscopic investigation under UV-illumination (g-
593 h). (3) Leaf Investigation after 60 min of US treatment: SEM micrographs (i-j) and stereomicroscopic
594 investigation under UV-illumination (k-l). PGT: Peltate Glandular Trichomes; NGT: Non-Glandular Trichomes;
595 ★ : rupture/opening zone.

596

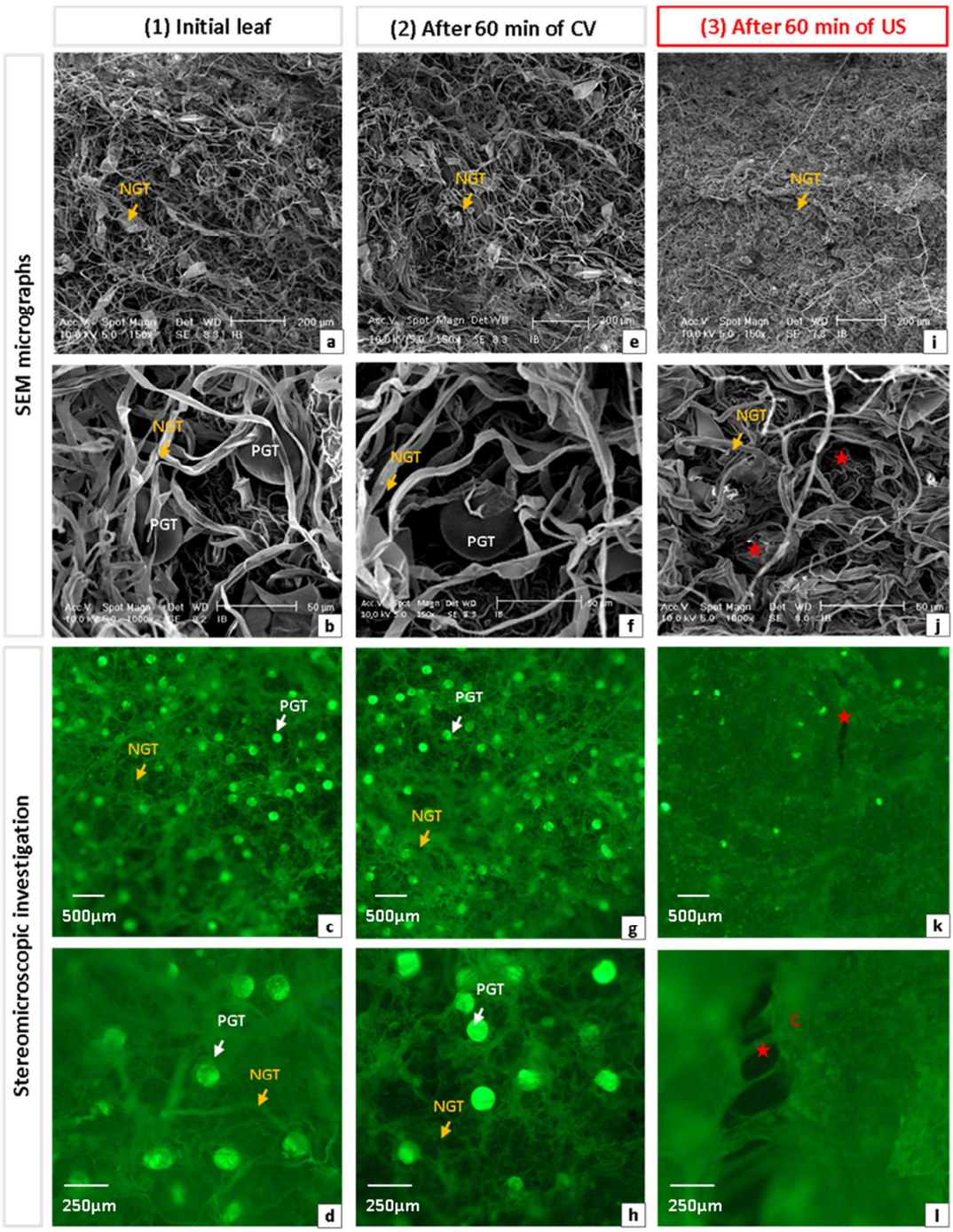

Figure 7. Investigation of *C. scolymus* abaxial leaf surface. (1) Investigation of the initial leaf: SEM micrographs (a-b) and stereomicroscopic investigation under UV-illumination (c-d). (2) Leaf Investigation after 60 min of CV procedure: SEM micrographs (e-f) and stereomicroscopic investigation under UV-illumination (g-h). (3) Leaf Investigation after 60 min of US treatment: SEM micrographs (i-j) and stereomicroscopic investigation under UV-illumination (k-l). PGT: Peltate Glandular Trichomes; NGT: Non-Glandular Trichomes; C: Abaxial Cuticle; ★ : rupture/opening zone.

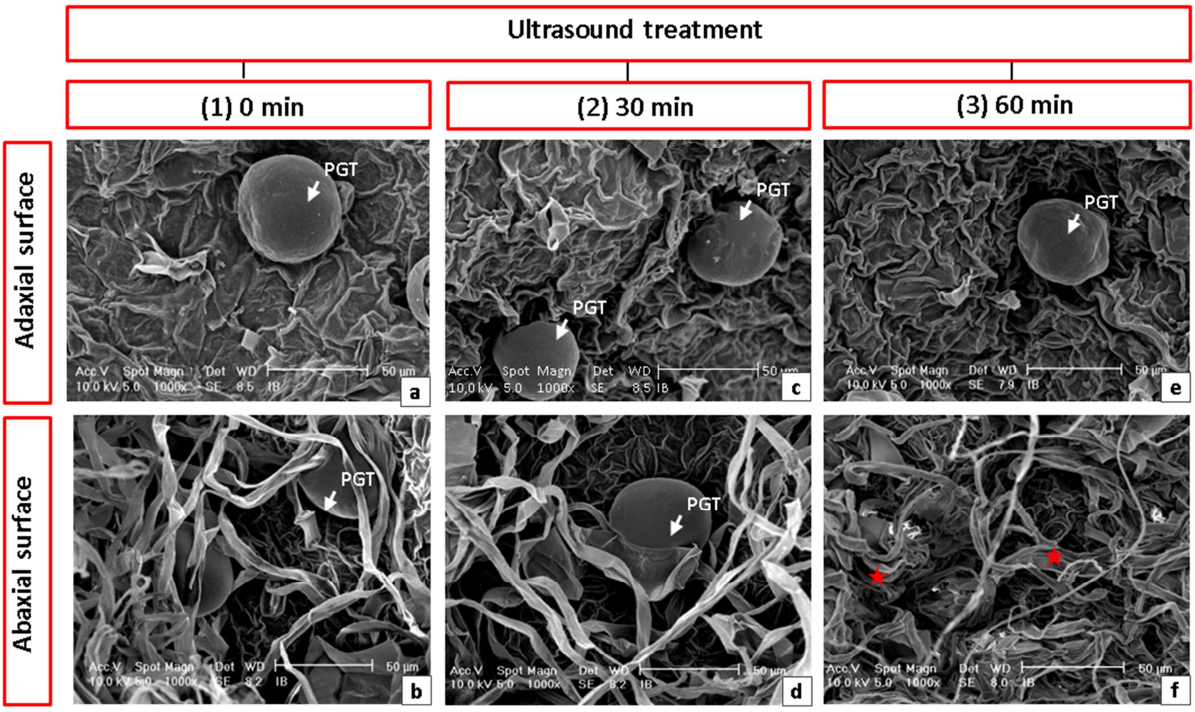

Figure 8. SEM micrographs of *C. scolymus* adaxial and abaxial surfaces during US treatment. (1) Initial leaf: adaxial surface (a) and abaxial surface (b). (2) After 30 min of ultrasounsd treatment: adaxial surface (c) and abaxial surface (d). (3) After 60 min of US treatment: adaxial surface (e) and abaxial surface (f)

IG: Internal Gland; ★ : rupture/opening zone.

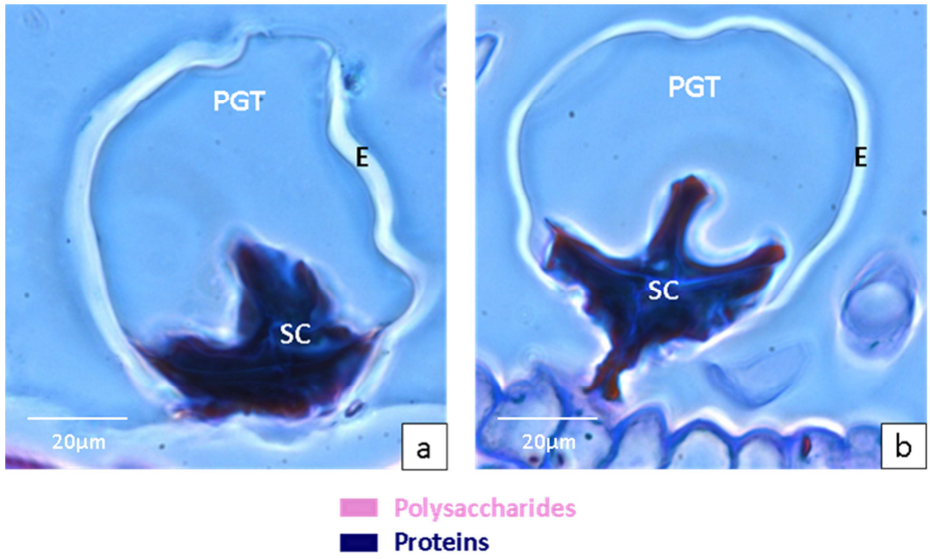

Figure 9. Cyto-histochemical investigation of *C. scolymus* PGT after staining with PAS/NBB reagent (phase contrast micrographs).

(a) Adaxial PGT. (b) Abaxial PGT.

PGT: Peltate Glandular Trichomes; SC: Secretory Cells; E: Storage cavity' envelope

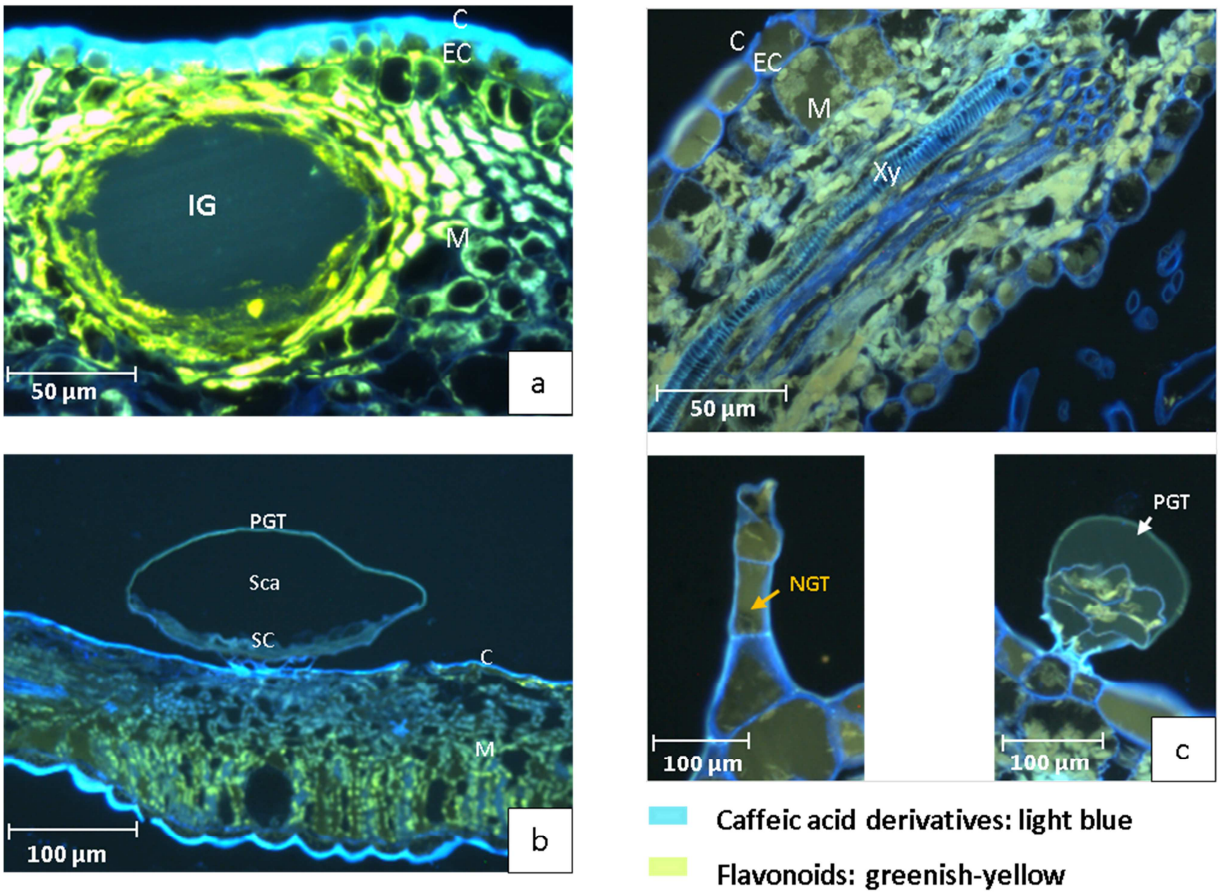

633

634 **Figure 10.** Cyto-histochemical study after revelation with Neu's reagent.

635 (a) *C. aurantium* leaf cross section. (b) *R. nigrum* leaf cross section. (c) *C. scolymus* leaf cross

636 section.

637 PGT: Peltate Glandular Trichomes; NGT: Non-Glandular Trichomes; Sca: Storage cavity;

638 SC: Secretory Cells; C: Cuticle; EC: Epidermal Cells; M: Mesophyll; Xy: Xylem

639

640

641

642

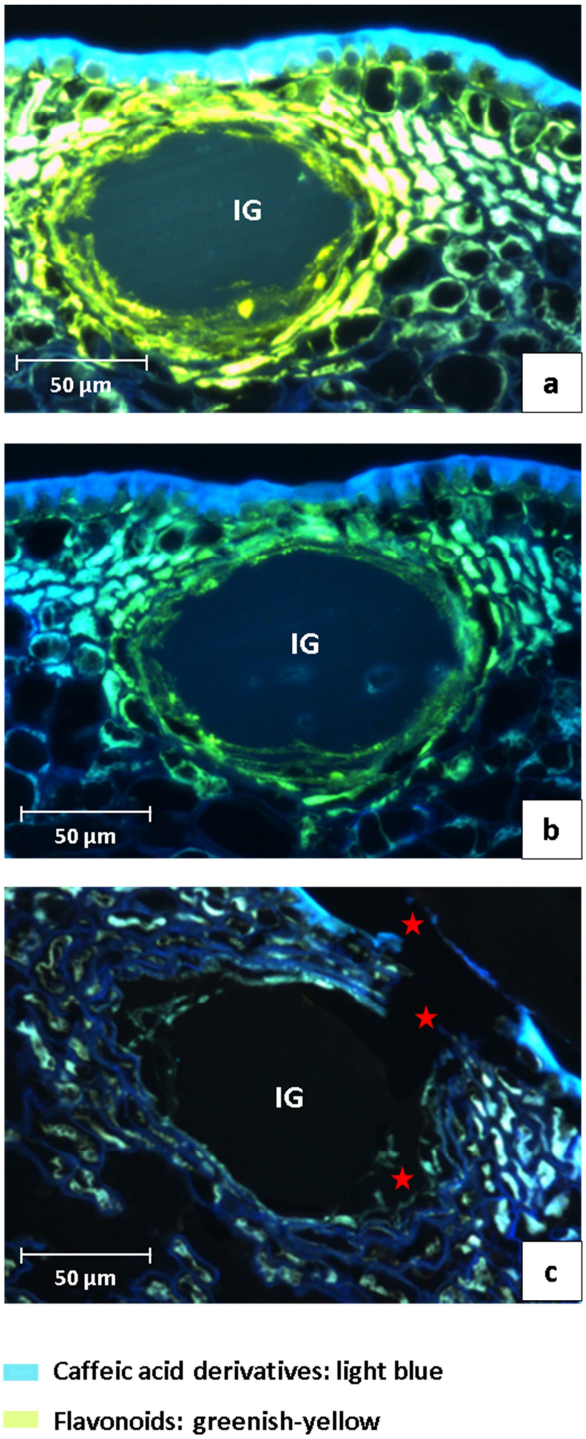

643

644 **Figure 11.** Cyto-histochemical study of *C. aurantium* adaxial leaf surface after staining with
645 Neu's reagent. (a) Initial leaf. (b) After 60 min of CV procedure. (c) After 60 min of US
646 treatment (UAE). IG: Internal Glands; ★: rupture zone

647